Spatial distribution of biogenic sulphur compounds (MSA, $nssSO_4^{2-}$) in the northern Victoria Land–Dome C–Wilkes Land area, East Antarctica

Silvia BECAGLI,[1] Marco PROPOSITO,[2] Silvia BENASSAI,[1] Roberto GRAGNANI,[2] Olivier MAGAND,[3] Rita TRAVERSI,[1] Roberto UDISTI[1]

[1]*Department of Chemistry, University of Florence, Via della Lastruccia 3, I-50019 Sesto Fiorentino (Florence), Italy*
E-mail: silvia.becagli@unifi.it
[2]*ENEA, Centro Ricerche Casaccia, PO Box 2400, I-00100 Rome, Italy*
[3]*Laboratoire de Glaciologie et Géophysique de l'Environnement (CNRS-UJF), 54 rue Molière, BP 96, 38402 Saint-Martin-d'Hères Cedex, France*

ABSTRACT. During the 1992–2002 Antarctic expeditions, in the framework of the International Trans-Antarctic Expedition (ITASE) project, about 600 sites were sampled (superficial snow, snow pits and firn cores) along traverses in the northern Victoria Land–Dome C–Wilkes Land region. The sites were characterized by different geographical (distance from the sea, altitude) and climatological (annual mean accumulation rate, temperature) conditions and were affected by air masses from different marine sectors (Ross Sea, Pacific Ocean). Mean anion and cation contents were calculated at each site, in order to evaluate the spatial distribution of chemical impurities in snow. Here we discuss the distribution of non-sea-salt sulphate ($nssSO_4^{2-}$) and of methanesulphonic acid (MSA) mainly originating from atmospheric oxidation of biogenic dimethyl sulphide; these compounds play a key role in climate control processes by acting as cloud condensation nuclei. The spatial distribution of $nssSO_4^{2-}$ and MSA is discussed as a function of distance from the sea, altitude and accumulation rate. Depositional fluxes of $nssSO_4^{2-}$ and MSA decrease as a function of distance from the sea, with a higher gradient in the first 200 km step. There is an analogous trend with the site altitude, and the first 1600 m step is relevant in determining the $nssSO_4^{2-}$ and MSA content in snow. The $nssSO_4^{2-}$/MSA ratio depends on the distance from the sea and the biogenic source strength. At coastal sites, where biogenic inputs are dominant, this ratio is ~2. As biogenic input decreases (low MSA content) inland, the ratio increases, indicating the presence of alternative sources of $nssSO_4^{2-}$ (crustal, volcanic background) or advection of low-latitude air masses. By plotting total flux as a function of accumulation rate, dry depositional contributions were evaluated for $nssSO_4^{2-}$ and MSA in the Ross Sea and Pacific Ocean sectors. Non-sea-salt sulphate wet deposition prevails at sites where the accumulation rate (expressed as water equivalent) is higher than 70 kg m^{-2} a^{-1} (Ross Sea sector) or 370 kg m^{-2} a^{-1} (Pacific Ocean sector). MSA threshold values in these sectors are respectively 90 and 220 kg m^{-2} a^{-1}.

1. INTRODUCTION

Knowledge of the spatial variability of the amount and chemical composition of recent snow precipitation in Antarctic coastal and central areas is essential in glacio-chemical studies assessing present-day atmospheric aerosol sources and their transport pathways. Such knowledge is needed to reliably interpret past variations in the chemical composition of snow recorded in ice cores. Several authors (e.g. Mulvaney and Wolff, 1994; Stenberg and others, 1998; Kreutz and Mayewski, 1999) have discussed the spatial variability of several chemical compounds in Antarctic snow as a function of geographical (altitude, distance from the sea) and climatological (temperature, snow accumulation rate) conditions at the sampling site, but knowledge of the chemical composition of snow in large areas of Antarctica is still lacking. High-resolution spatial records of chemical compounds in snow precipitation are essential in understanding the chemical–physical processes affecting net depositional fluxes of species useful as climatic and environmental markers. These records are also essential in evaluating the role of several parameters affecting the origin, transformation, transport, deposition and preservation of chemical compounds in snow.

Sulphuric acid (H_2SO_4, measured in snow as non-sea-salt sulphate ($nssSO_4^{2-}$)) and methanesulphonic acid (MSA), the main components of sulphur-oxidized compounds, play a key role in controlling the climate of remote marine areas since they represent the greatest source of cloud condensation nuclei (Charlson and others, 1987). In uncontaminated oceanic and coastal regions, H_2SO_4 and MSA mainly arise from the atmospheric oxidation of their precursor dimethyl sulphide (DMS). DMS is emitted into the atmosphere through the metabolic processes of phytoplankton (Saltzman, 1995). Recent studies have proposed MSA as a marker of past sea-ice extent by a positive correlation between changes in MSA concentrations in coastal ice cores and local sea-ice cover variations (Curran and others, 2003), which are in turn controlled by anomalies in southern atmospheric circulation (Southern Oscillation Index) (Kwok and Comiso, 2002).

MSA may allow the reconstruction of past oceanic phytoplanktonic productivity in the last glacial–interglacial climate cycles (Legrand and others, 1991). However, this

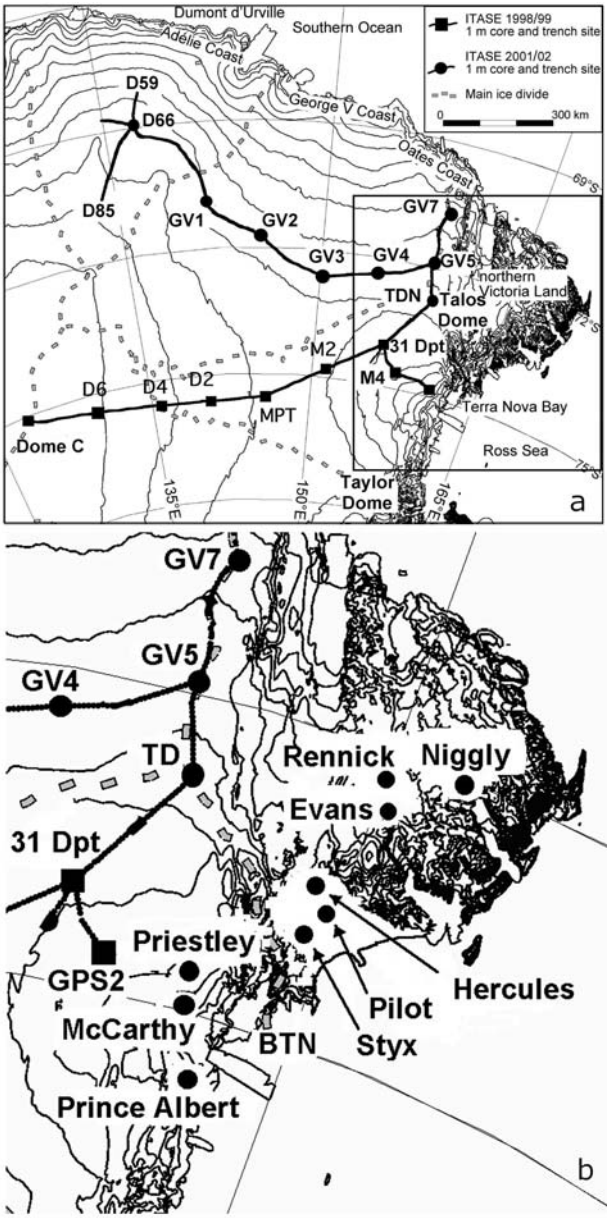

Fig. 1. Map of the sampled area. Squares refer to the 1998/99 ITASE traverse; dots indicate snow-pit sites sampled during the 2001/02 ITASE traverse and in the northern Victoria Land region. Contour line interval is 250 m.

role was recently questioned because at sites with low accumulation rates, MSA is heavily affected by post-depositional processes that significantly change its original concentration (Wagnon and others, 1999; Udisti and others, 2004; Weller and others, 2004). In any case, because of their great importance in controlling climatic and environmental processes, it is necessary to increase our knowledge of the spatial and temporal distribution of $nssSO_4^{2-}$ and MSA. To correctly interpret changes in snow concentration and depositional fluxes recorded in ice-core stratigraphies, we must understand transport and depositional processes of these compounds.

In this paper, we show an extensive mapping of the distribution of $nssSO_4^{2-}$ and MSA depositional fluxes in the northern Victoria Land (NVL)–Dome C (DC)–Dumont d'Urville (DdU) East Antarctic sector. The dataset was created by calculating mean values for surface snow and firn (from snow pits and firn cores) samples collected from about 600 sites. Particular attention was paid in interpreting flux variations as a function of altitude and distance from the sea, and in evaluating the wet and dry relative contributions in coastal and central sites. The spatial distribution of the $nssSO_4^{2-}$/MSA ratio was also studied, in order to understand fractionation effects, probably occurring during transport or caused by different depositional processes (Udisti and others, 1998).

2. SAMPLING AND ANALYSIS

In the framework of the ITASE (International Trans-Antarctic Scientific Expedition), Station Concordia (French–Italian collaboration) and PNRA (Programma Nazionale di Ricerche in Antartide) programmes, about 600 sites were sampled during the 1992/93 to 2001/02 Antarctic expeditions in the NVL–DC–DdU region. Sampling sites are shown in Figure 1 and Table 1. At each site, several samples of surface snow and/or firn from snow pits and shallow firn cores were collected. Details of sampling and chemical analysis were reported in previous papers (Udisti and others, 1998, 1999; Frezzotti and Flora, 2002; Proposito and others, 2002; Becagli and others, 2003, 2004).

A total of five shallow firn cores (5–50 m) were drilled and 27 snow pits (1.5–7 m) were excavated in the study area. Firn cores were subsampled with a mean resolution of 5.0 cm after decontamination by removing a ~1 cm external layer with a stainless-steel scraper. Subsamples were stored at –20°C until analysis. Snow-pit samples were collected at 2.5–3 cm resolution. Pit walls were cleaned by removing a 5–10 cm snow layer with a stainless-steel scraper just before sampling. Pre-cleaned polypropylene vials were inserted into the vertical snow walls; after removal, each sampling vial was labelled and sealed in a double polyethylene bag. Snow density was determined along the pit wall by collecting horizontal core sections with a known volume and weighing them immediately after retrieval.

A total of 590 1 m integrated surface snow samples were collected with a hand auger along the ITASE traverses (1998/99 and 2000/01 Antarctic expeditions) and sealed in polyethylene bags. Samples were stored at –20°C, decontaminated by removing an external layer of about 1 cm with a stainless scraper, and melted just before analysis.

All snow pits, firn cores and 1 m integrated superficial snow samples were analyzed by ion chromatography (IC) for their ionic content. Two IC instruments were used in parallel to determine major cations (Na^+, NH_4^+, K^+, Mg^{2+}, Ca^{2+}) and anions (Cl^-, NO_3^-, SO_4^{2-}, F^- and MSA). A detailed description of analytical methods is given by Gragnani and others (1998) and Udisti and others (2004). Here we discuss only the spatial distribution of mean $nssSO_4^{2-}$ and MSA fluxes calculated at each site. All the mean data are related to the uppermost layers, corresponding to different time periods at the different sites, as a function of depth and accumulation rate. For the firn cores and snow pits, we usually calculated the mean concentration in snow layers approximately representing deposition over the last 3–40 years. Since firn cores and snow pits were sampled during different Antarctic summer expeditions, deposition periods do not coincide. Table 1 shows the time periods over which mean values were calculated for each sampling site. Mean values were calculated for three snow pits (sampled during different expeditions) at Dome C, in order to evaluate the spatial variability of MSA and $nssSO_4^{2-}$ deposition at a

Table 1. Snow pits and firn-core sites. Time period refers to the time range from the sampling year used for MSA and $nssSO_4^{2-}$ mean calculation. Time was calculated by stratigraphic dating or (at Dome C) from the surface to deposition year of Pinatubo eruption (see text for explanation)

Site, sampling type (Antarctic campaign)	Lat. (S)	Long. (E)	Elevation m a.s.l.	Distance from sea km	Time period years
GPS2 snow pit (1998/99)	74°38.69′	157°30.13′	1776	167	5
31Dpt snow pit (1998/99)	74°01.52′	155°57.6′	2065	238	5
M2 snow pit (1998/99)	74°48.27′	151°16.17′	2308	327	~14*
Mid point (MPT) snow pit (1998/99)	75°32.16′	145°51.43′	2454	460	~27*
D2 snow pit (1998/99)	75°37.33′	140°37.84′	2611	587	~22*
D4 snow pit (1998/99)	75°35.88′	135°49.89′	2792	692	~40*
D6 snow pit (1998/99)	75°26.85′	129°48.53′	3024	851	~40*
Dome C snow pit (1997/98)	75°06′	123°21′	3233	1000	5
Dome C snow pit (1998/99)	75°06′	123°21′	3233	1000	6
Dome C snow pit (2001/02)	75°06′	123°21′	3233	1000	8
D66 snow pit (2001/02)	68°56.38′	136°56.112′	2333	280	3
GV1 snow pit (2001/02)	70°52.27′	141°23.00′	2244	400	4
GV2 snow pit (2001/02)	71°42.70′	145°15.786′	2143	395	3
GV3 snow pit (2001/02)	72°37.7′	150°10.433′	2137	450	4
GV4 snow pit (2001/02)	72°23.32′	154°29.05′	2126	330	3
GV5 snow pit (2001/02)	71°53.22′	158°32.216′	2184	200	3
GV7 snow pit (2001/02)	70°41.05′	158°51.749′	1947	95	3
Talos Dome snow pit (2001/02)	72°46.24′	159°04.545′	2316	250	4
Talos Dome firn core (1996/97)	72°46.24′	159°04.545′	2316	250	5
Priestley Névé snow pit (1993/94)	73°38.3′	160°38.5′	1983	120	3
Rennick Glacier snow pit (1993/94)	73°14.84′	162°29.060′	2310	220	5
McCarthy Ridge snow pit (1993/94)	74°36.00′	163°03.131′	850	40	3
McCarthy Ridge firn core (1992/93)	73°51.94′	163°41.715′	1660	50	5
Styx Glacier snow pit (1993/94)	73°51.94′	163°41.715′	1660	50	6
Styx Glacier firn core (1991/92)	73°51.94′	163°41.715′	1660	50	5
Hercules Névé snow pit (1993/94)	73°06.38′	165°27.785′	2960	90	5
Hercules Névé firn core (1992/93)	73°06.38′	165°27.785′	2960	90	5
Pilot Glacier snow pit (1993/94)	73°15.85′	163°30.772′	2100	60	5
Prince Albert snow pit (1993/94)	75°10.30′	162°07.53′	800	40	3
Niggly Névé snow pit (1993/94)	72°41.15′	166°58.1′	2610	120	5
Evans Névé snow pit (1996/97)	74°42.2′	166°56.4′	2520	140	5

*Estimated on the basis of the mean accumulation rate from Frezzotti and others (2004).

site involved in deep ice-core drilling (European Project for Ice Coring in Antarctica; see, e.g., EPICA community, 2004). Since stratigraphic dating was not possible at Dome C due to the low accumulation rate, mean values were calculated over time periods ranging between the sampling year (younger limit) and the Pinatubo (Philippines) signatures (older limit). In Antarctic snow, the Pinatubo eruption (AD 1991) is recorded in the 1991–93 deposition layers. Sulphate volcanic spikes were removed before calculating the mean in order to discriminate the biogenic input.

Accumulation rates used in flux calculations were measured (firn cores and snow pit) or estimated (1 m integrated samples) at each sampling site.

Beta-tritium peaks from 1965–66 thermonuclear atmospheric bomb tests were used to calculate the mean accumulation rate at the firn-core drilling sites sampled during the 1998/99 and 2000/01 ITASE traverses (Frezzotti and others, 2004; Magand and others, 2004). Mean accumulation rates in northern Victoria Land snow-pit sampling sites were calculated using a multiparametric dating method based on the chemical stratigraphy of seasonal markers (MSA, $nssSO_4^{2-}$, H_2O_2) (Udisti, 1996; Stenni and others, 2000).

Accumulation rates at the 590 sites where 1 m integrated samples were collected were evaluated through accumulation-rate vs 15 m temperature, or accumulation-rate vs longitude relationships.

At each main site along the Terra Nova Bay (TNB)–DC traverse, three shallow firn cores were drilled at points showing the highest, the intermediate and the lowest accumulation rate, as revealed by the stratigraphy of radar reflector layers. Frezzotti and others (2004) suggested that the accumulation rate measured in the area showing the highest accumulation rate and flat snow-surface topography is representative of snow precipitation at the site, because wind-driven snow erosion or redistribution processes are minimum or absent. At these sites, Frezzotti and others (2004) found an excellent correlation ($R = 0.92$) between maximum snow accumulation values from core data and firn temperatures at 15 m depth. Using literature data, Frezzotti and others (2004) also confirmed the close correlation ($R = 0.97$) between accumulation rate and 15 m temperature at high-accumulation sites along the DdU–DC transect. Two different linear regressions were used to evaluate snow accumulation at each 1 m integrated sample site (every 5 km) along the TNB-DC traverse and the DdU–DC transect.

The same approach was also applied to the GV7–Talos Dome transect, where a good correlation ($R = 0.93$) was found between β-counting accumulation rate and 15 m temperature (Magand and others, 2004).

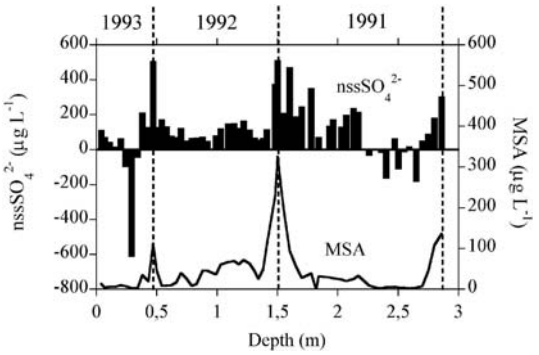

Fig. 2. $NssSO_4^{2-}$ and MSA concentration/depth profiles from McCarthy Ridge snow pit.

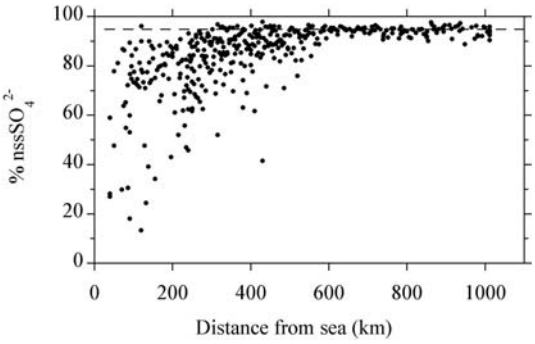

Fig. 3. Percentage contribution of $nssSO_4^{2-}$ with respect to total SO_4^{2-} reported as a function of distance from the sea.

In contrast, along the west–east (D66–GV5) transect, there is no linear correlation between β-counting accumulation rate and 15 m temperature (Magand and others, 2004). However, a clear trend was observed between β-counting accumulation rate and longitude (Magand and others, 2004, fig. 3b). Along this transect, the snow accumulation rate in each 1 m core site was therefore evaluated through a linear regression between two consecutive checkpoints (sites where the accumulation rate was calculated using β-counting) on either side of it.

3. RESULTS AND DISCUSSION

Calculation of $nssSO_4^{2-}$

The $nssSO_4^{2-}$ contribution is usually calculated using total Na as sea-spray marker. Here, for better accuracy, $nssSO_4^{2-}$ was evaluated from the $ssNa^+$ fraction according to the equation:

$$nssSO_4^{2-} = SO_4^{2-} - 0.253 ssNa^+,$$

where SO_4^{2-} is the total sulphate concentration and $ssNa^+$ is the Na^+ actually derived from sea spray. Since some Na^+ derives from continental dust, $ssNa^+$ was calculated using the four-equation system reported below and knowing total Na^+, total Ca^{2+}, the mean Ca^{2+}/Na^+ ratio in the crust ($(Na^+/Ca^{2+})_{crust} = 1.78$ w/w; Bowen, 1979) and the mean Ca^{2+}/Na^+ ratio in sea water ($(Ca^{2+}/Na^+)_{seawater} = 0.038$ w/w; Bowen, 1979).

$$ssNa^+ = Na^+ - nssNa^+$$
$$nssNa^+ = nssCa^{2+}(Na^+/Ca^{2+})_{crust}$$
$$nssCa^{2+} = Ca^{2+} - ssCa^{2+}$$
$$ssCa^{2+} = ssNa^+(Ca^{2+}/Na^+)_{seawater}$$

In all the analyzed samples, the contribution of $nssNa^+$ is usually <20%, but it reaches a significantly higher percentage in stations more affected by crustal-enriched aerosol components (Benassai and others, 2005). The mean theoretical ratio of SO_4^{2-}/Na^+ (w/w) in sea water is 0.253. Wagenbach and others (1998) suggested that the bulk sea-water ratio at Antarctic coastal sites was variable because of SO_4^{2-} fractionation processes due to the formation of frost flowers on fresh sea ice and the subsequent precipitation of mirabilite ($Na_2SO_410H_2O$) at temperatures below –8.2°C; this leads to a decrease in the SO_4^{2-}/Na^+ ratio of primary marine aerosol. The $ssSO_4^{2-}$component is overestimated if one considers a bulk sea-water ratio of 0.253; this determines negative $nssSO_4^{2-}$ values in winter sea-spray deposition occurring at sites where $nssSO_4^{2-}$ inputs are significantly lower than $ssSO_4^{2-}$, i.e. coastal sites. Indeed, we found negative $nssSO_4^{2-}$ values only at McCarthy Ridge station, located at a low altitude (850 m a.s.l.) and near the sea (40 km). Figure 2 shows the $nssSO_4^{2-}$ profile in the 3 m deep snow pit dug at McCarthy Ridge, together with the profile of MSA, used as a seasonal marker (summer peaks). In the 3 years of deposition, negative $nssSO_4^{2-}$ values are recorded in two fall periods, just after the summer MSA peaks.

Rankin and others (2002) showed that frost flowers formed on the surface of fresh sea ice by volatilization–condensation processes are depleted in SO_4^{2-} due to the precipitation of mirabilite, and that these may constitute a major source of sea-spray aerosol, at least for coastal sites. The contribution of frost-flower aerosol was evident during some fall seasons in only one of the investigated sites. The contribution of this aerosol to the global budget of annual sea-spray deposition in areas located at different distances from the sea and at different altitudes is not quantifiable. For this region we adopted a SO_4^{2-}/Na^+ ratio of 0.253 in our $nssSO_4^{2-}$ calculation.

Geographical variability

Figure 3 reports the $nssSO_4^{2-}$ percentage as a function of distance from the sea. The $nssSO_4^{2-}$ percentage is low at stations nearest to the sea and progressively increases with distance from the sea, reaching a stable value of around 95% at 600 km inland. This pattern is attributed to atmospheric scavenging of primary aerosol particles by wet and dry removal processes. Indeed, sea-spray components (such as $ssSO_4^{2-}$) are mainly distributed on super-micrometric particles having relatively short atmospheric residence times with respect to the secondary components (such as sub-micrometric particles arising from gas-to-particle conversion of biogenic gaseous emissions) (e.g. Minikin and others, 1998; Udisti and others, 1998; Becagli and others, 2003; Traversi and others, 2004).

To evaluate the spatial distribution of S-cycle secondary components, $nssSO_4^{2-}$ and MSA concentrations are usually plotted as a function of distance from the coast and/or altitude. In areas affected by very different accumulation rates, where the relative contribution of wet and dry removal is variable, the depositional flux seems to be a more reliable parameter than concentration in evaluating the spatial distribution of impurities in snow. Atmospheric aerosol loads can be correctly reconstructed from depositional fluxes only in areas where dry deposition is dominant

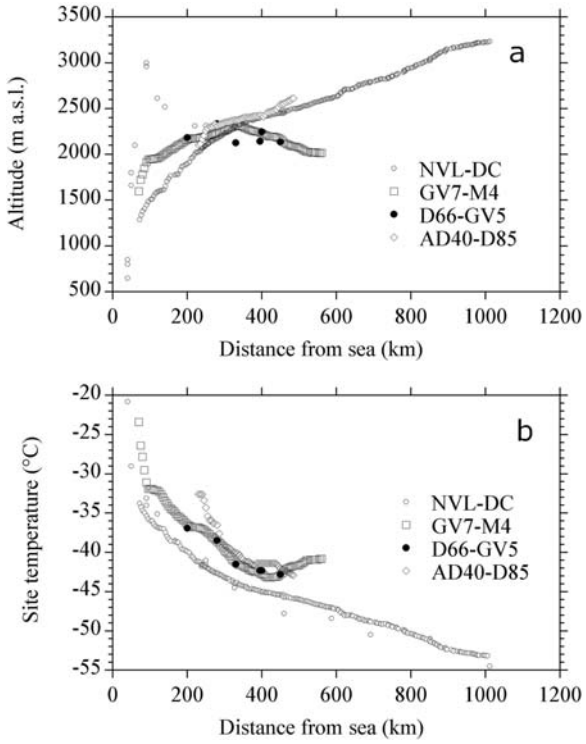

Fig. 4. Altitude (a) and site temperature (b) reported as a function of distance from the sea in the studied areas.

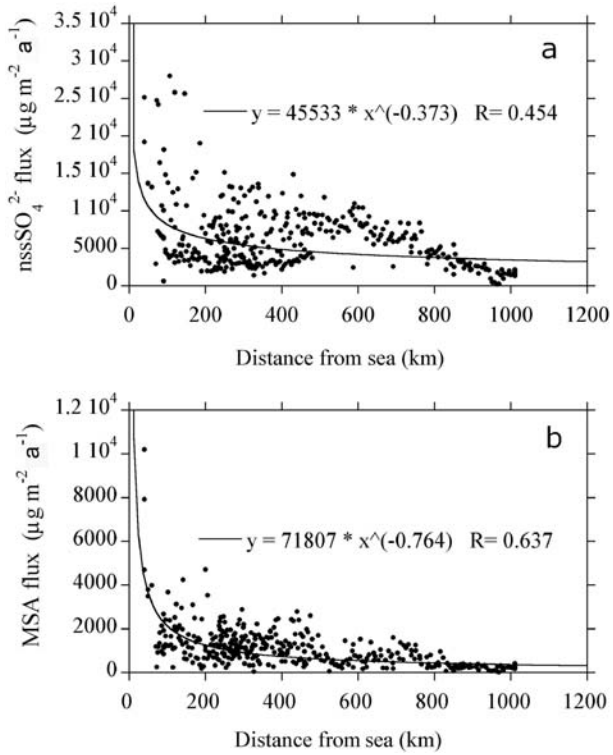

Fig. 5. $NssSO_4^{2-}$ (a) and MSA (b) depositional fluxes reported as a function of distance from the sea.

(Mayewski and Legrand, 1990; Udisti and others, 2004). On the other hand, wet deposition controls atmospheric scavenging processes in coastal areas, making fluxes positively correlated with accumulation rates (Legrand and Delmas, 1987; Fischer and Wagenbach, 1996). As a consequence, it is important to accurately assess the relative contribution of dry and wet deposition in the sampling areas in order to effectively calculate the atmospheric load.

Total (wet and dry) MSA and $nssSO_4^{2-}$ depositional fluxes are calculated by multiplying snow ion concentration ($\mu g\,L^{-1}$) by the mean annual accumulation rate ($kg\,m^{-2}\,a^{-1}$):

$$F = CA(\mu g\,m^{-2}\,a^{-1}, \text{ considering snow melted density} = 1),$$

where F_{tot} is total wet and dry deposition flux, C is snow ion concentration and A is mean snow accumulation rate.

The distance from the aerosol source, and changes in altitude and mean temperature are the main factors affecting the snow composition at coastal and central Antarctic sites. Since these three parameters are correlated, it is not easy to clearly evaluate their individual contribution. Altitude and distance from the sea are usually positively correlated moving inland from the Antarctic coast, and temperature is inversely correlated with altitude. The highest altitude gradients occur in the first 200 km inland, both in the NVL–DC transect (empty circles in Fig. 4) and in the Pacific sector (empty squares, empty rhomb and dots in Fig. 4). These sharp changes control the atmospheric load and chemical composition of aerosol.

Since altitude and distance from the sea are positively correlated, both can be used to interpret changes in the deposition pattern of chemical species. Sampling sites along transects are evenly spaced from coastal to inland areas, regardless of altitude. Indeed, the altitude in the examined region changes dramatically in the first 200 km inland step, remaining quite constant for the following 800 km or so. For this reason, in order to clearly discern patterns, we chose distance from the sea, instead of altitude, as the reference parameter for evaluating spatial trends in the chemical composition of snow in the NVL–DC–DdU sector. In Figure 4a and b, altitude and temperature are plotted as a function of distance from the sea. We used distance from the coastline as 'distance from the sea' in order to avoid uncertainties linked to seasonal variations in sea-ice extent. Indeed, primary (sea-spray) and secondary (biogenic) marine components show opposite seasonal patterns: sea spray peaks in winter, while biogenic compounds show summer maxima. This evidence reveals that changes in source intensity and transport processes are dominant with respect to changes in the distance air masses have to cover over sea ice.

When plotted against distance from the sea (Fig. 5a and b), $nssSO_4^{2-}$ and MSA depositional fluxes show a dramatic decrease in the first 100 km, well before the altitude (or temperature) gradient decreases.

This pattern highlights the first 1500 m step, which is a critical threshold for the inland penetration of secondary atmospheric aerosols. From coastal values as high as $3\times10^4\,kg\,m^{-2}\,a^{-1}$ ($nssSO_4^{2-}$) or $1\times10^4\,kg\,m^{-2}\,a^{-1}$ (MSA), the fluxes drop to values one order of magnitude lower in the first 100 km inland. However, we note that this decrease in flux is lower than that of sea-spray components (Udisti and others, 1998, 1999; Benassai and others, 2005) according to the different size classes in which primary and secondary aerosol particles are distributed. From 100 km inland towards the interior, $nssSO_4^{2-}$ and MSA fluxes show a much slower tendency to decrease, reaching values of around 1600 and 200 $kg\,m^{-2}\,a^{-1}$ respectively in the Dome C area (1100 km inland, 3200 m a.s.l.). The overall pattern can be

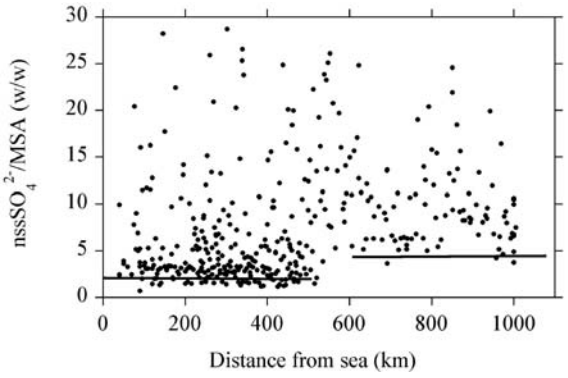

Fig. 6. $NssSO_4^{2-}$/MSA (w/w) ratio reported as a function of distance from the sea. Lines in the plot represent the limit values (see text for explanation).

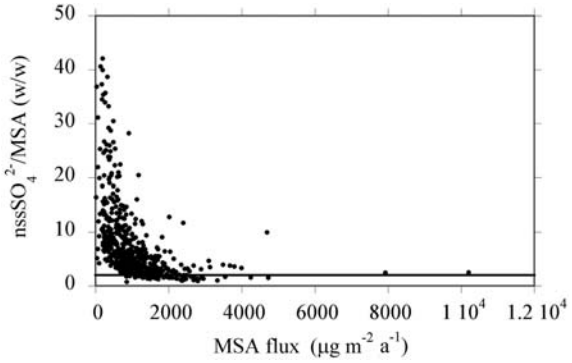

Fig. 7. $NssSO_4^{2-}$/MSA (w/w) ratio reported as a function of MSA depositional fluxes. The line in the plot represents the limit value.

modelled by a power function whose fit-curves and equations are shown in Figure 5a and b.

While an exponential function seems to fit the MSA pattern (Fig. 5b), the $nssSO_4^{2-}$ trend is less accurately described. By using a second- or third-order polynomial fit we obtained slightly higher regression coefficients (0.500 instead of 0.454); however, the modelled trend has no physical interpretation, giving negative $nssSO_4^{2-}$ fluxes for distances >950 km from the sea. The unsatisfactory exponential fitting of the $nssSO_4^{2-}$ flux pattern in the 400–700 km inland range (Fig. 5a) could be due to changes in the contribution of various sources (biogenic, crustal, volcanic, low-latitude transport, etc.) to the total $nssSO_4^{2-}$ budget, especially in a distance range where a boundary layer occurs between prevailing wet and dry depositional processes (see below). By contrast, MSA shows a good exponential fit due to its univocal biogenic source.

The trends of $nssSO_4^{2-}$ and MSA fluxes as a function of distance from the sea are qualitatively similar but quantitatively different, showing the possible effects of fractionation processes occurring during inland transport or different wet/dry contributions during atmospheric removal. In order to highlight these different patterns, the $nssSO_4^{2-}$/MSA ratio was plotted as a function of distance from the sea (Fig. 6). Although data are relatively scattered, two evident thresholds limit the lower $nssSO_4^{2-}$/MSA ratios. In the first 400 km, the lowest ratios reach values of around 2 (Fig. 6) and are similar to those measured in fresh summer precipitations in coastal areas ($nssSO_4^{2-}$/MSA = 2.7; Udisti and others, 1998). This threshold therefore seems to be determined by precipitation characterized by a high marine, biogenic contribution possibly in relation to local or regional transport. The trend of the $nssSO_4^{2-}$/MSA ratio as a function of MSA flux (Fig. 7) supports this hypothesis. The $nssSO_4^{2-}$/MSA ratio reaches low, constant values of around 2 for high MSA fluxes, i.e. in coastal stations where the biogenic contribution is higher. As the distance from the sea increases, the lower limit of the $nssSO_4^{2-}$/MSA ratio (Fig. 6) increases to about 4.5.

This increase starts about 450 km inland, where the temperature/distance gradient (i.e. the slope of the temperature curve shown in Fig. 4b) becomes constant. This pattern could be attributed to MSA-$nssSO_4^{2-}$ fractionation during transport due to the different contribution of dry and wet deposition. The MSA shows higher solubility in water than SO_4^{2-}. Indeed, Henry's law constant is higher for MSA ($k_H = 6.5\times10^{13}$) than for sulphuric acid ($k_H = 8.74\times10^{10}$) (Brimblecombe, 1996), which is the original acidic gaseous species of biogenic $nssSO_4^{2-}$ in the atmosphere. Henry's law constant k_H is defined as $k_H = C_{H_2O}/p_{gas}$, where C_{H_2O} is the concentration of a chemical species in the aqueous phase and p_{gas} is the partial pressure of the same species in the gas phase. The values reported here refer to standard conditions (temperature = 298.15 K). Since MSA is more hygroscopic than $nssSO_4^{2-}$, gas-to-particle conversion processes (when gaseous MSA reacts with atmospheric moisture) are more efficient in MSA, leading to the formation of a larger number of cloud condensation nuclei (O'Dowd and others, 1997). As a consequence, MSA should be mainly distributed in cloud micro-droplets and be more prone than sulphate to wet removal as temperature decreases. This hypothesis is confirmed by contemporaneous snow/aerosol measurements at Dome C, where the MSA/SO_4^{2-} ratio is higher in snow than in atmospheric particulate, indicating more effective wet scavenging (Udisti and others, 2004). The MSA distribution on more accreted (by atmospheric moisture absorption) particles is also demonstrated by size-segregated aerosol measurements at Dome C carried out using an eight-stage impactor (10–0.4 μm range): MSA shows two clear size modes in the 1.1–2.1 and 0.4–0.7 μm range, while sulphate is mainly distributed in the 0.4–0.7 μm size range (Fattori and others, 2004).

Another reason for the increasing $nssSO_4^{2-}$/MSA ratio in central Antarctic areas could be related to the advection of air masses from lower latitudes. Higher SO_4^{2-}/MSA ratios are caused by temperature-dependent atmospheric oxidation pathways of phytoplanktonic DMS from lower latitudes (Bates and others, 1992).

Wet and dry contributions to net depositional fluxes

The net depositional flux of an airborne substance can be considered as the sum of three contributions (Fischer and Wagenbach, 1996):

$$F_{tot} = F_d + F_w + \Delta F\,, \qquad (1)$$

where F_d and F_w are the dry and wet deposition fluxes, and ΔF represents the effect of post-depositional processes able to change the original composition of precipitation. For irreversibly deposited species like SO_4^{2-}, the term ΔF can be disregarded. In contrast, MSA undergoes post-depositional processes (mainly re-emission into the atmosphere of gaseous MSA species from the snow surface or migration

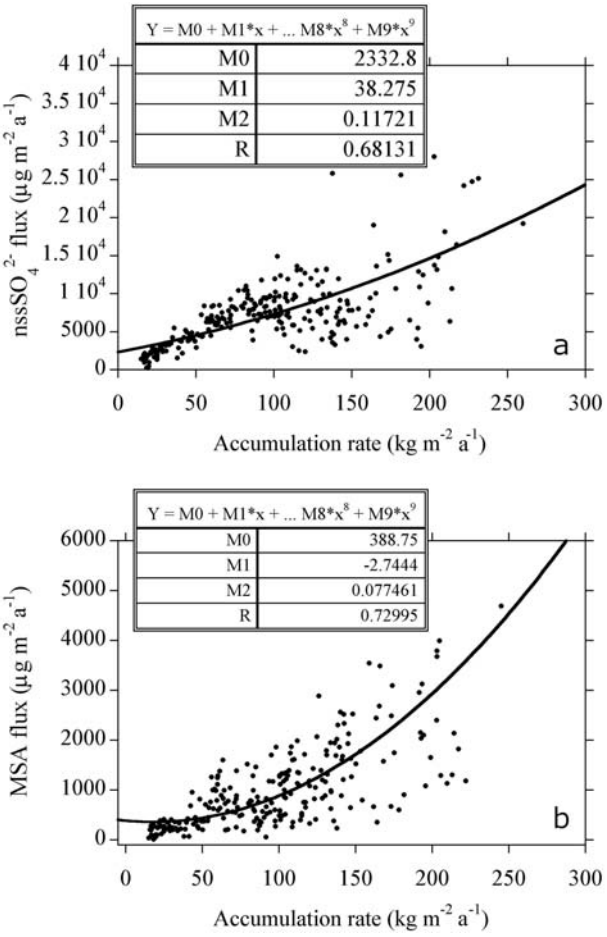

Fig. 8. $NssSO_4^{2-}$ and MSA depositional fluxes reported as a function of accumulation rate in the Ross Sea sector.

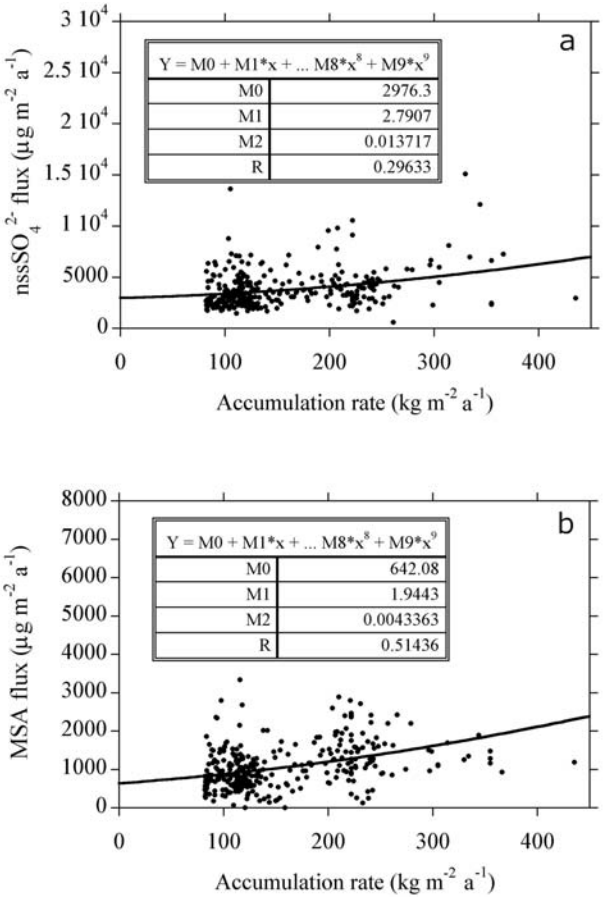

Fig. 9. $NssSO_4^{2-}$ and MSA depositional fluxes reported as a function of accumulation rate in the Pacific Ocean sector.

in firn layers) at low-accumulation sites (Wagnon and others, 1999; Weller and others, 2004). Snow-pit measurements at Dome C, where the accumulation rate is among the lowest measured in the present work, revealed that the decrease in MSA with depth was not visible in the uppermost layers, but required about 5 m depth to be accomplished. MSA summer-to-winter movements highlighted by Pasteur and Mulvaney (2000) do not affect the multi-year mean. Since we consider superficial snow layers covering several years, we assume that post-depositional processes play a minor role in MSA depositional flux evaluation.

For each chemical component, the wet deposition flux is calculated as

$$F_w = C_p A\,, \tag{2}$$

where C_p is the concentration associated with wet deposition and A is the accumulation rate. Considering ΔF as negligible and taking into account Equation (2):

$$F_{tot} = F_d + C_p A\,. \tag{3}$$

Fischer and Wagenbach (1996) assume C_p as a constant for moist air masses generating snow precipitation along pathways from source areas to inland deposition sites. By plotting F_{tot} as a function of accumulation rates measured at each site, they obtained a linear regression whose intercept represents the contribution of the dry depositional flux.

However, the extensive dataset reported here shows that a simple linear model inadequately explains the pattern of total flux as a function of accumulation rate in every sector. Figures 8 and 9 show the relationships linking $nssSO_4^{2-}$ (plot A) and MSA (plot B) fluxes with accumulation rate for all 600 reported sites, separating the stations mainly affected by Ross Sea inputs (NVL–DC; Fig. 8) from those affected by the greater influence of the Pacific Ocean (Fig. 9). Although data are largely scattered, second-order polynomial regressions seem to describe the trends better than linear regressions, at least in the NVL–DC sector. Assuming that F_d is independent of the accumulation rate, the relationship between F_{tot} and accumulation rate is expressed by the generic equation

$$F_{tot} = F_d + M1A + M2A^2\,.$$

In particular,

$$F_{tot} = 2330 + 38.3A + 0.12A^2$$
$$(R = 0.68)\ nssSO_4^{2-} \text{ in the Ross Sea sector}$$

$$F_{tot} = 390 - 2.7A + 0.08A^2$$
$$(R = 0.73)\ \text{MSA in the Ross Sea sector}$$

$$F_{tot} = 2980 + 2.8A + 0.01A^2$$
$$(R = 0.30)\ nssSO_4^{2-} \text{ in the Pacific Ocean sector}$$

$$F_{tot} = 640 + 1.9A + (4.3 \times 10^{-3})A^2$$
$$(R = 0.51)\ \text{MSA in the Pacific Ocean sector.}$$

The relatively high second-order coefficients for the Ross Sea sector, together with the high correlation coefficients,

support the polynomial model for this area. As in the case of the relationship between $nssSO_4^{2-}$ fluxes and distance from the sea, the interpretation of $nssSO_4^{2-}$ flux trends with respect to accumulation rate is not straightforward. The slightly higher correlation coefficient ($R = 0.75$) obtained for a third-order polynomial regression, involving very negative values (physically unexplainable) as accumulation rate tends to zero, prevents evaluation of the dry deposition contribution.

The trends obtained by the second-order polynomial fitting suggest that the concentration of wet precipitation is higher ($C_p = M1 + M2A$) in areas where the accumulation rate is high, i.e. in coastal regions very near to sources of secondary marine aerosol. The lower values found for the Pacific Ocean sector show that a linear model should be used (C_p may be considered constant).

The high $nssSO_4^{2-}$ and MSA fluxes measured at Ross Sea coastal sites (with high accumulation rates) and their fast decrease inland highlight the high biogenic productivity in the region (possibly related to the larger extension of annual sea-ice cover; Curran and others, 2003) and reveal how the sharp increase in elevation results in a decrease in the atmospheric aerosol load through wet deposition. The Pacific Ocean sector shows a more homogeneous pattern due to the lower intrusion of atmospheric moisture correlated with the persistence of higher atmospheric pressure in the central portion of the transect between sites GV2 and GV4 (Magand and others, 2004).

The second-order polynomial regressions drawn in Figures 8 and 9 allow a good estimation of the F_d contribution, calculated as Y-intercept values (accumulation rate = 0). Non-sea-salt sulphate shows dry depositional fluxes of 2330 and 2980 $\mu g\,m^{-2}\,a^{-1}$ in the Ross Sea and Pacific Ocean sectors, respectively. The corresponding MSA values are 390 and 640 $\mu g\,m^{-2}\,a^{-1}$. Based on the critical accumulation rate, defined as the accumulation rate for which $F_w = F_d$ (i.e. total flux $= 2F_d$), we can roughly determine sites in each sector where dry deposition is the primary depositional process. MSA and $nssSO_4^{2-}$ dry deposition dominates areas in the Ross Sea sector with accumulation rates lower than 90 and 70 $kg\,m^{-2}\,a^{-1}$ respectively. The corresponding values for the Pacific Ocean sector are 220 and 370 $kg\,m^{-2}\,a^{-1}$ for MSA and $nssSO_4^{2-}$ respectively. The large difference between critical values in the Ross Sea and Pacific Ocean sectors could be in part due to the lower significance of the Pacific Ocean sector correlation ($R = 0.51$ and $R = 0.30$ respectively), although differences in atmospheric circulation also play an important role. Indeed, Magand and others (2004) suggested that the intrusion of atmospheric moisture and the penetration of synoptic cyclonic systems are less effective in the Pacific Ocean sector due to the persistence of high atmospheric pressure in the central portion of this region. As a result, air masses controlling precipitation in this area have already undergone fractionation by wet deposition.

4. CONCLUSIONS

The spatial distribution of depositional fluxes of biogenic S-oxidized compounds ($nssSO_4^{2-}$ and MSA) in recent snow at coastal and central Antarctic sites (NVL–DC–DdU sector) is highly dependent on geographical position (altitude and distance from the sea). Flux as a function of distance from the sea and of accumulation rate, instead of concentration, seems to be the best parameter for describing $nssSO_4^{2-}$ and MSA depositional trends along coast-inland traverses. The different $nssSO_4^{2-}$ and MSA flux patterns are interpreted by observing trends in the $nssSO_4^{2-}$/MSA ratio as a function of distance from the sea and of MSA content (as a specific biogenic marker). The increase in the $nssSO_4^{2-}$/MSA ratio with distance from the sea reflects the more efficient scavenging of atmospheric MSA by wet deposition; this evidence is supported by the high Henry constant (about three orders of magnitude higher than that of $nssSO_4^{2-}$), indicating the greater affinity of MSA for the liquid phase. In addition, as the MSA flux decreases (i.e. at lower biogenic inputs), the $nssSO_4^{2-}$/MSA ratio increases exponentially. This suggests $nssSO_4^{2-}$ contributions from alternative sources (crustal, volcanic background). Alternatively, this trend could be due to the long-range transport of marine air masses less enriched in MSA from lower latitudes. At sites with a high MSA content, the $nssSO_4^{2-}$/MSA ratio approaches 2, a value similar to that found in fresh summer snow sampled at coastal sites (2.7; Udisti and others, 1998). This value is therefore assumed to identify precipitation supplied by local-to-regional air masses enriched in MSA (summer, high-latitude sources).

$NssSO_4^{2-}$ and MSA dry deposition in the Ross Sea sector, estimated by plotting fluxes vs accumulation rate, is dominant at sites with accumulation rates lower than 70–90 $kg\,m^{-2}\,a^{-1}$. In the Pacific Ocean sector, dry deposition dominates at sites with accumulation rates lower than 220–370 $kg\,m^{-2}\,a^{-1}$. This is in agreement with the pattern of atmospheric circulation; indeed, the intrusion of atmospheric moisture and the penetration of synoptic cyclonic systems are less effective in this sector due to the persistence of high atmospheric pressure in the central areas, roughly corresponding to the central portion of the D66–GV5 transect (Magand and others, 2004). This pattern limits the contribution of wet deposition, thereby increasing the accumulation rate threshold value for dry/wet deposition.

Knowledge of the present wet/dry relative contribution of chemical compounds in snow allows better interpretation of changes recorded in ice-core stratigraphies, distinguishing changes driven by variations in source intensity or transport processes from those induced by changes in accumulation rate.

ACKNOWLEDGEMENTS

This research was financially supported by the MIUR (Ministero Istruzione, Università, Ricerca)–PNRA programme through a cooperation agreement among the PNRA consortium, Milano-Bicocca University and Venice University in the framework of the 'Glaciology' and 'Environmental Contamination' projects. This work is an Italian contribution to the ITASE project. It is a contribution to the 'European Project for Ice Coring in Antarctica' (EPICA), a joint European Science Foundation/European Commission (EC) scientific programme, funded by the EC and by national contributions from Belgium, Denmark, France, Germany, Italy, the Netherlands, Norway, Sweden, Switzerland and the United Kingdom. This is EPICA publication No. 143.

REFERENCES

Bates, T.S., J.A. Calhoun and P.K. Quinn. 1992. Variations in the methanesulfonate to sulfate molar ratio in submicrometer marine aerosol particles over the south Pacific Ocean. *J. Geophys. Res.*, **97**(D9), 9859–9865.

Becagli, S. *and 6 others*. 2003. Variability of snow depositions along the 1998/99 ITASE traverse. *Terra Antarctica Reports,* **8**, 43–48.

Becagli, S. *and 12 others*. 2004. Chemical and isotopic snow variability in East Antarctica along the 2001/02 ITASE traverse. *Ann. Glaciol.,* **39**, 473–482.

Benassai, S. *and 7 others*. 2005. Sea-spray deposition in Antarctic coastal and plateau areas from ITASE traverses. *Ann. Glaciol.,* **41** (see paper in this volume).

Bowen, H.J.M. 1979. *Environmental chemistry of the elements*. London, Academic Press.

Brimblecombe, P. 1996. *Air composition and chemistry*. Cambridge, Cambridge University Press.

Charlson, R.J., J.E. Lovelock, M.O. Andreae and S.G. Warren. 1987. Oceanic phytoplankton, atmospheric sulphur, cloud albedo and climate. *Nature,* **326**(6114), 655–661.

Curran, M.A.J., T.D. van Ommen, V.I. Morgan, K.L. Phillips and A.S. Palmer. 2003. Ice core evidence for Antarctic sea ice decline since the 1950s. *Science,* **302**(5648), 1203–1206.

EPICA community. 2004. Eight glacial cycles from an Antarctic ice core. *Nature,* **429**(6992), 623–628.

Fattori, I., S. Bellandi, S. Benassai, M. Innocenti, A. Mannini and R. Udisti. 2004. Ion balances of size resolved aerosol samples from Terra Nova Bay and Dome C (Antarctica). In Colacino, M., *ed. 10th Workshop on Italian Research on Antarctic Atmosphere and SCAR Workshop on Oceanography, Rome, 22–24 October 2003*. Bologna, Italian Physical Society, 101–115.

Fischer, H. and D. Wagenbach. 1996. Large-scale spatial trends in recent firn chemistry along an east–west transect through central Greenland. *Atmos. Environ.,* **30**(19), 3227–3238.

Frezzotti, M. and O. Flora. 2002. Ice dynamic features and climatic surface parameters in East Antarctica from Terra Nova Bay to Talos Dome and Dome C: ITASE Italian traverses. *Terra Antartica,* **9**(1), 47–54.

Frezzotti, M. *and 12 others*. 2004. New estimations of precipitation and surface sublimation in East Antarctica from snow accumulation measurements. *Climate Dyn.,* **23**(7–8), 803–813.

Gragnani, R., C. Smiraglia, B. Stenni and S. Torcini. 1998. Chemical and isotopic profiles from snow pits and shallow firn cores on Campbell Glacier, northern Victoria Land, Antarctica. *Ann. Glaciol.,* **27**, 679–684.

Kreutz, K.J. and P.A. Mayewski. 1999. Spatial variability of Antarctic surface snow glaciochemistry: implications for paleoatmospheric circulation reconstructions. *Antarct. Sci.,* **11**(1), 105–118.

Kwok, R. and J.C. Comiso. 2002. Southern Ocean climate and sea ice anomalies associated with the Southern Oscillation. *J. Climate,* **15**(5), 487–501.

Legrand, M. and R.J. Delmas. 1987. A 220-year continuous record of volcanic H_2SO_4 in the Antarctic ice sheet. *Nature,* **327**(6124), 671–676.

Legrand, M., C. Feniet-Saigne, E.S. Saltzman, C. Germain, N.I. Barkov and V.N. Petrov. 1991. Ice-core record of oceanic emissions of dimethylsulphide during the last climate cycle. *Nature,* **350**(6314), 144–146.

Magand, O., M. Frezzotti, M. Pourchet, B. Stenni, L. Genoni and M. Fily. 2004. Climate variability along latitudinal and longitudinal transects in East Antarctica. *Ann. Glaciol.,* **39**, 351–358.

Mayewski, P.A. and M. Legrand. 1990. Recent increase in nitrate concentration of Antarctic snow. *Nature,* **346**(6281), 258–260.

Minikin, A. *and 7 others*. 1998. Sulfur-containing species (sulfate and methanesulfonate) in coastal Antarctic aerosol and precipitation. *J. Geophys. Res.,* **103**(D9), 10,975–10,990.

Mulvaney, R. and E.W. Wolff. 1994. Spatial variability of the major chemistry of the Antarctic ice sheet. *Ann. Glaciol.,* **20**, 440–447.

O'Dowd, C.D., M.H. Smith, I.E. Consterdine and J.A. Lowe. 1997. Marine aerosol, sea-salt, and the marine sulphur cycle: a short review. *Atmos. Environ.,* **31**(1), 73–80.

Pasteur, E.C. and R. Mulvaney. 2000. Migration of methane sulphonate in Antarctic firn and ice. *J. Geophys. Res.,* **105**(D9), 11,525–11,534.

Proposito, M. *and 9 others*. 2002. Chemical and isotopic snow variability along the 1998 ITASE traverse from Terra Nova Bay to Dome C, East Antarctica. *Ann. Glaciol.,* **35**, 187–194.

Rankin, A.M., E.W. Wolff and S. Martin. 2002. Frost flowers: implications for tropospheric chemistry and ice core interpretation. *J. Geophys. Res.,* **107**(D23), 4683. (doi: 10.1029/2002JD002492.)

Saltzman, E.S. 1995. Ocean/atmosphere cycling of dimethylsulfide. *In* Delmas, R.J., *ed. Ice core studies of global biogeochemical cycles*. Berlin, etc., Springer-Verlag, 65–90. (NATO ASI Series I: Global Environmental Change 30.)

Stenberg, M. *and 7 others*. 1998. Spatial variability of snow chemistry in western Dronning Maud Land, Antarctica. *Ann. Glaciol.,* **27**, 378–384.

Stenni, B. *and 6 others*. 2000. Snow accumulation rates in northern Victoria Land, Antarctica, by firn-core analysis. *J. Glaciol.,* **46**(155), 541–552.

Traversi, R. *and 7 others*. 2004. Spatial and temporal distribution of environmental markers from coastal to plateau areas in Antarctica by firn core chemical analysis. *Int. J. Environ. Anal. Chem.,* **84**(6–7), 457–470.

Udisti, R. 1996. Multiparametric approach for chemical dating of snow layers from Antarctica. *Int. J. Environ. Anal. Chem.,* **63**, 225–244.

Udisti, R., R. Traversi, S. Becagli and G. Piccardi. 1998. Spatial distribution and seasonal pattern of biogenic sulphur compounds in snow from northern Victoria Land, Antarctica. *Ann. Glaciol.,* **27**, 535–542.

Udisti, R., S. Becagli, E. Castellano, R. Traversi, S. Vermigli and G. Piccardi. 1999. Sea-spray and marine biogenic seasonal contribution to snow composition at Terra Nova Bay, Antarctica. *Ann. Glaciol.,* **29**, 77–83.

Udisti, R. *and 7 others*. 2004. Atmosphere–snow interaction by a comparison between aerosol and uppermost snow layers composition at Dome C, East Antarctica. *Ann. Glaciol.,* **39**, 53–65.

Wagenbach, D. *and 7 others*. 1998. Sea-salt aerosol in coastal Antarctic regions. *J. Geophys. Res.,* **103**(D9), 10,961–10,974.

Wagnon, P., R.J. Delmas and M. Legrand. 1999. Loss of volatile acid species from upper firn layers at Vostok, Antarctica. *J. Geophys. Res.,* **104**(D3), 3423–3431.

Weller, R., F. Traufetter, H. Fischer, H. Oerter, C. Peel and H. Miller. 2004. Post-depositional losses of methane sulfonate nitrate and chlorine at the EPICA deep-drilling site in Dronning Maud Land, Antarctica. *J. Geophys. Res.,* **109**(D7), D07301. (10.1029/2003JD004189).